ISSN: 2776-0960 Volume 3, Issue 9 Sep., 2022

ResearchJet Journal of Analysis and Inventions
https://reserchjet.academiascience.org

SIMULATION AND STUDY OF MESO-METALLOPORPHYRIN ELECTRONIC PROPERTIES BY USING A DFT LOGARITHMS

Ashraq T. Atwan
Physics Department, Science College, Thi-Qar University, Nassiriya – Iraq.
*Corresponding Author: E-mail: ashraq522@gmail.com

Mohammed L. Jabbar
Physics Department, Science College, Thi-Qar University, Nassiriya – Iraq.

Abstract

Some porphyrins and their metal complex (metalloporphyrin) play significant roles in sensing, photodynamic therapy, magnetic resonance imaging (MRI), anticancer drugs, electronic devices, and fluorescence imaging. In this study, the effect of changing the central metal was taken into consideration, as titanium metal and cadmium metal were used. In addition to adding chlorine atoms to the central metal, as well as studying the effects of different ends of the compound, once by making hydrogen at the meso-ends and again by making phenol rings at the meso-ends. And knowledge of all previous effects on electronic properties and their improvement. For example, the energy of filled and empty orbitals, the energy gap, hardness, softness chemical electronegativity, and electrophilicity are calculated. It can be seen that the selected materials have a lower energy gap than the original porphyrin. This result is very important. The energy gap of the compounds studied, all of which are located in the semiconducting region (1.109352 - 2.91692 eV), can therefore be used in important electronic applications such as sensors and solar cells. All calculations were carried out with the Gaussian 09 software package and in accordance with the density functional theory.

Keywords: porphyrin; density functional theory; energy gap; metals; infrared spectra

1. Introduction

In recent decades, porphyrin have proven their economic feasibility in the manufacture and development of most electronic devices and the possibility of

ResearchJet Journal of Analysis and Inventions
https://researchjet.academiascience.org

using them in electronic devices present and in the future[1,2] . A porphyrin is a big ring molecule made up of four pyrroles[1,3], which are smaller rings consisting of four carbons and one nitrogen. These pyrrole molecules are linked by a sequence of single and double bonds, forming a huge ring. A tetra-pyrrole is the technical name for four pyrroles linked together[4–9]. The ring has a very even distribution of electrons around its diameter. As a result, a porphyrin is classified as an aromatic chemical. A porphyrin molecule is extremely stable in this state. Porphin is the model of a generic porphyrin[10]. This molecule is only encountered as an intermediate in nature very seldom, but it is the foundation of all porphyrin molecules. The last research in porphyrin is two-dimensional compounds (i.e., the rings are flat in space) or three-dimensional[11], in which there are many studies at the level of theoretical research[7,12–16] and practical research[17–20] to understand and obtain physical properties that can be applied in electronic technologies. Metalloporphyrins have been employed as powerful catalysts in a wide range of chemical processes [8,21–25]. sensing, photodynamic therapy (PDT), magnetic resonance imaging (MRI),anticancer drugs, eletronic devices, and fluorescence imaging because of their preferential selective approval and retention via tumor tissues[5,26].

The electronic structure properties of the ground state of the metalloporphyrin were carried out theoretical by using the first principle in the density functional theory DFT computations the first principle.The values of HOMO, LUMO energies, forbidden energy values, Fermi level ionization potential, electronic affinity, electronegativity (χ), electrophilicity (ω), and electrostatic potential were studied, as well as group electronic properties, resulting in IR spectra.

2. Computational Details

Porphyrin is an organic compound. It is structurally composed of four pyrrole rings connected to each other by diagonal bridges in a closed fashion to form a huge ring at the end. It is the simplest tetrapyrrole compound, which is a solid aromatic compound[5]. Current theoretical calculations have been investigated utilizing the first principle computation in the density functional theory (DFT)[27–29]. Whereas the geometry optimization was achieved using the B3LYP model[30]. These symbols refer to Becke's three parameters Lee-Yang-Parr also is called the hybrid functional[31–33], which is considered an excellent

ResearchJet Journal of Analysis and Inventions
https://reserchjet.academiascience.org

choice to investigate the optimization in the light of DFT. The 6-31G basis set was used quantum chemical computation[34,35].

All systems could be relaxed before energy investigations for porphyrin and metalloporphyrin (porphyrin with metals both Titanium (Ti) and Cadmium (Cd) atoms). This process is termed "geometry optimization." The electronic properties of porphyrin include the energy of the Fermi level, the highest occupied molecular orbital (HOMO) energies, the lowest unoccupied molecular orbital (LUMO) energies, and energy gaps (the difference between the eigenvalues of the maximum valence band and the minimum conduction band or by mathematically expressed [27,36–38]:

$$E_g = E_{LUMO} - E_{HOMO} \qquad (1)$$

Structures are studied theoretically with involve of Ti and Cd impurities. According to Koopman's approximation in which the frontier orbital energies are given by the following relationship[29,39,40]

$$I.P. = -HOMO\ E.A. = -LUMO\ \} \qquad (2)$$

Subsequently, the ionization potential (I.P) and electron affinity (E.A) values can be used to determine electronegativity, hardness, softness, and electrophilicity.

Mulliken electronegativity (χ) is an index that describes the tendency or power of a functional group or an atom in a structure to attract electrons [29,38,40]:

$$\chi = \frac{I.P+E.A}{2} \qquad (3)$$

The global hardness was proposed by Parr and Pearson define

$$\eta = \frac{1}{2}\left(\frac{\partial^2 E}{\partial N^2}\right)_V \qquad (4)$$

After simplifying the equation 4 can be rewritten as

$$\eta = \frac{I.P-E.A}{2} \qquad (5)$$

Also, global softness is defined by the reverse of hardness by the following relationship

$$\sigma = \frac{1}{2\eta} \qquad (6)$$

The electrophilicity index is defined as

$$\omega = \frac{\chi^2}{2\eta} = \frac{(I.P+E.A)^2}{4(I.P-E.A)} \qquad (7)$$

Finally, the Fermi level can be written as

ResearchJet Journal of Analysis and Inventions
https://reserchjet.academiascience.org

$$F_L = \frac{E_{HOMO}+E_{LUMO}}{2} \qquad (8)$$

3. Results and Discussion

In the first stage, the shape of porphyrin was designed, including 20 carbon atoms, 4 nitrogen and hydrogen atoms. The carbon atoms are built as rings of a quad lattice. The structure of porphyrin treated with hydrogen passivation decreases the boundary effects. Subsequently, the structure is treated until it reaches the best position for stability. This process is called geometry optimization. However, we did not observe the apparent deformation of pristine porphyrin and their directions. The preceding certainly agrees with figure 1.

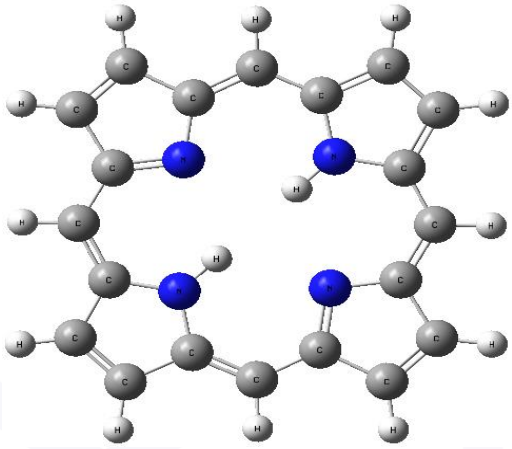

Figure 1. Geometry optimization of pure porphyrin

The second stage is the addition of some impurities to the pristine porphyrin to get a new enhanced property such as electronic, optical, mechanical, and several properties. The pristine structure is doped by Titanium (Ti) and Cadmium (Cd) atoms. All these structures are clearly shown in figure 2, which involves Titanium meso-tetra (4-hydrogen) porphyrin (TiTHP), Titanium-Chlore meso-tetra (4-hydrogen) porphyrin (TiClTHP), Titanium meso-tetra(4-phenyl)porphyrin (TiTPP), Cadmium meso-tetra(4-hydogen)porphyrin (CdTHP), Cadmium-Chlore meso-tetra(4-hydogen) porphyrin (CdClTHP), and Cadmium meso-tetra(4-phenyl) porphyrin (CdTPP). It is important to visualize that the simulation for all the structures is performed using the DFT method with the B3LYP hybrid functional in the light of the Gaussian 09 software package[41]. Eventually, the vibrational spectrum is calculated without imaginary wavenumbers. This result confirms that the structures deduced correspond to minimum energy.

ResearchJet Journal of Analysis and Inventions
https://reserchjet.academiascience.org

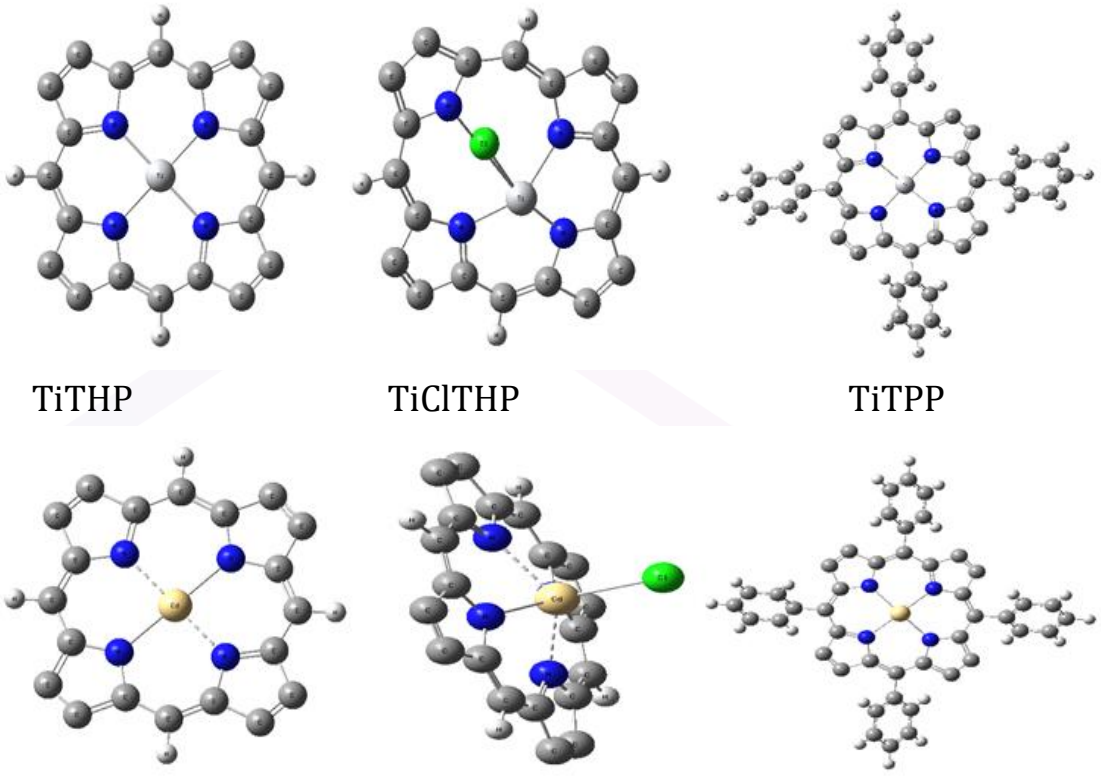

Figure 2: geometry optimization of metalloporphyrin in different sites where Ti, Cd, and Cl represent Titanium, Cadmium, and chlorine atoms, respectively.

There are two kinds of stretching oscillations: symmetric and asymmetrical. When similar atoms stretch in the same direction, this is referred to as symmetric stretching. When they oscillate in the same phase, asymmetric stretching is happening when the bonds oscillate in a variety of phases. Infrared spectra yield harmonics vibrational frequencies. Low frequencies give torsion vibrations. The number of atomic modes depends on the number of atoms in the molecule. Elastic or inelastic vibration can occur.

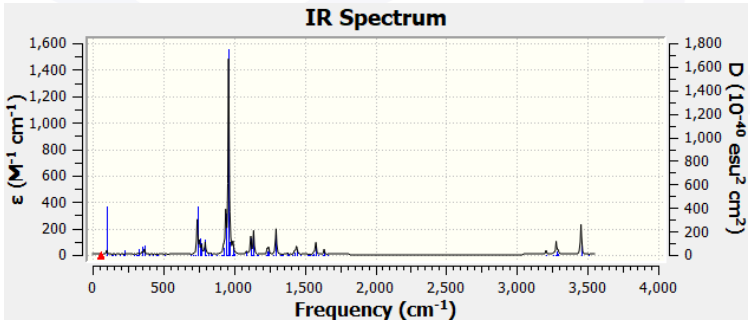

Porphyrin

ResearchJet Journal of Analysis and Inventions
https://reserchjet.academiascience.org

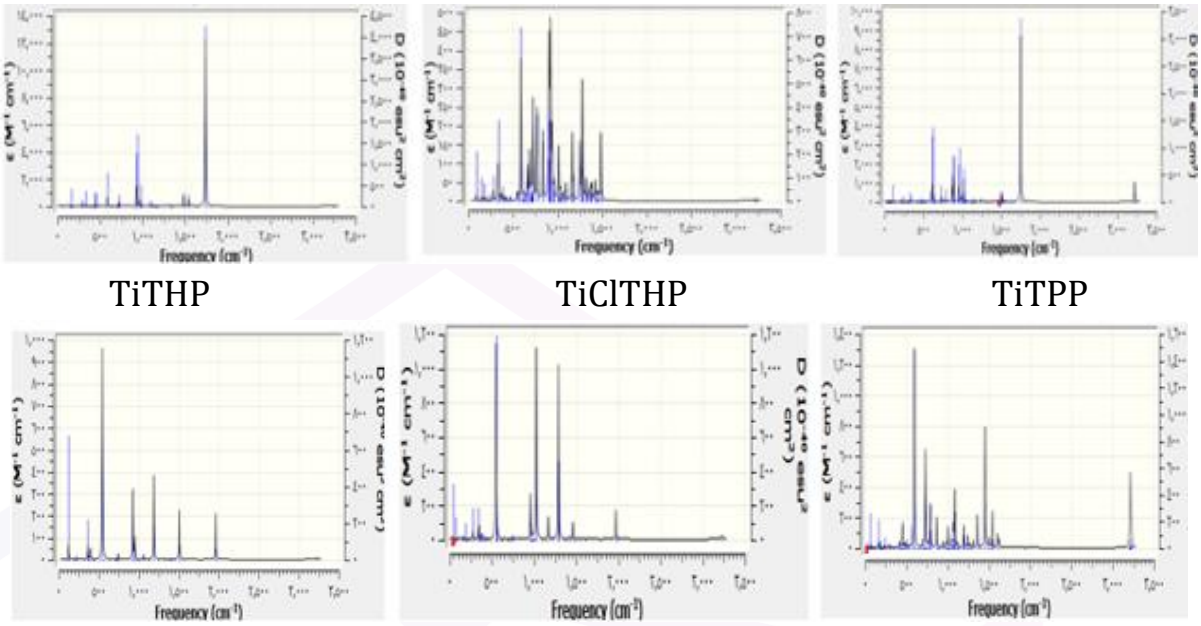

Figure3. the infrared spectra of all structure such as porphyrin and metalloporphyrin (metals are Ti, Cd)

Figure 3 elucidates that there are other pinnacles. Each pinnacle represents a bond between two neighboring particles, whereas the results are in good agreement with experimental data[2,5]. All charts of the infrared spectra have peaks between approximately 650-1000 cm^{-1}, these peaks are attributed to the vibrations and absorption of carbon atoms with double bonds. Moreover, it contains peaks with a frequency of 1640 cm^{-1}, which results from the vibration of bonds between carbon and nitrogen atoms. The other peaks represent the presence of other impurity atoms such as metal (Ti, Cd) and chlorine atoms.

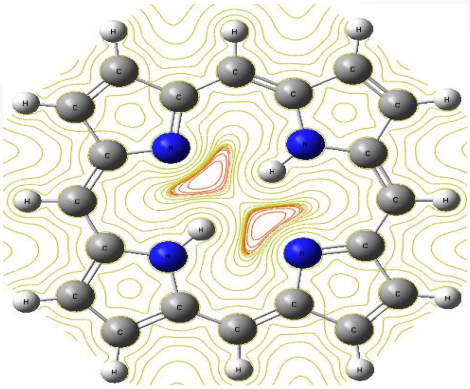

Porphrin

ResearchJet Journal of Analysis and Inventions
https://reserchjet.academiascience.org

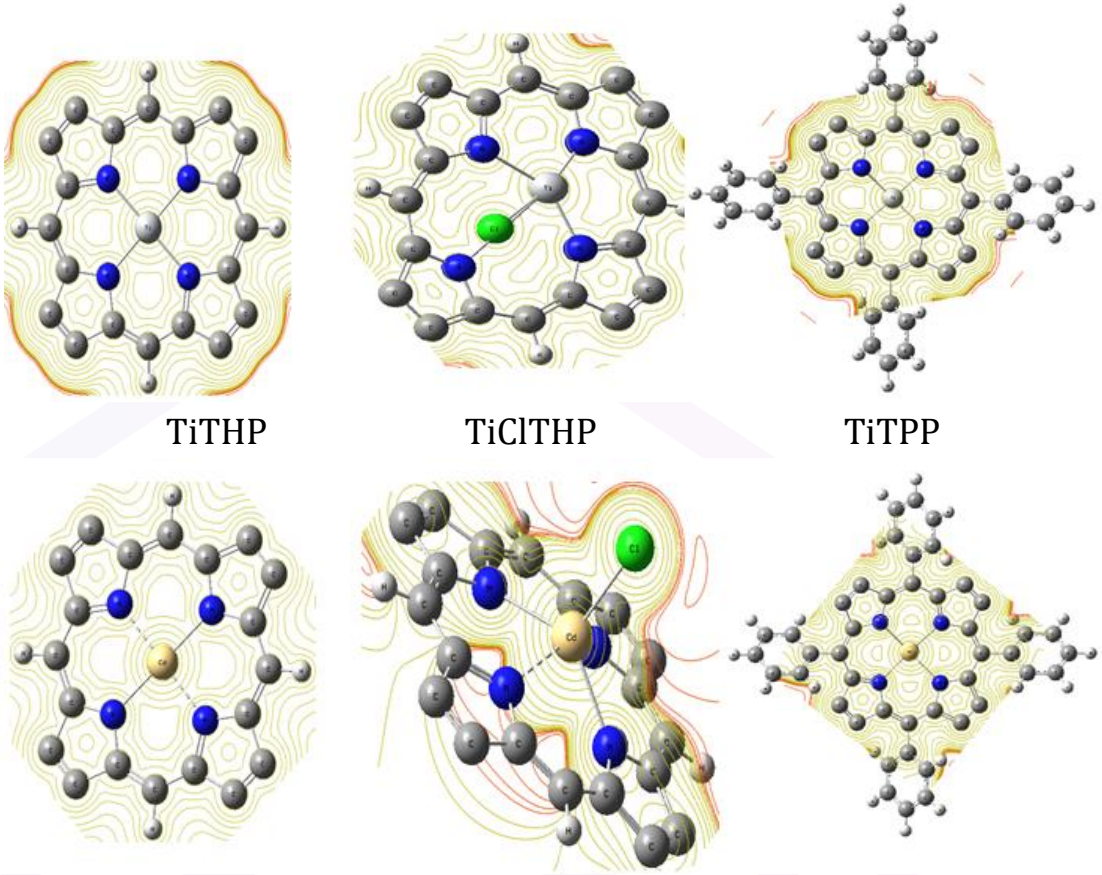

Figure 4. Electrostatic potential (ESP) contour map of porphyrin and metalloporphyrins, respectively.

The electrostatic potential (ESP) contour map has been plotted over the Mulliken charge density for structures of porphyrin and metalloporphyrins, respectively. As shown in Figure 4. Through the distribution of the charge (in Figure 4), we can note that the pure compound porphyrin has a distortion in the distribution of negative charges, so it appears in red in the center of the compound, while the rest of the compounds, that is, after adding the metal to the porphyrin (metalloporphyrin), are more stable and the distribution of the charge is more uniform, so the Berillion zones are on the The shape of semi-regular circles is not significantly distorted. This may be attributed to the amount of positive and negative charges present in the compound, in addition to their density of distribution in the compound. Finally, the central circle is between the carbon atoms. These circles represent the regions of Brillion, where the first central

ResearchJet Journal of Analysis and Inventions
https://reserchjet.academiascience.org

circle represents the zone of the first Brillion. And the second circle represents the second Brillion zone, and so on with the other bands. Naturally, the electrons in the first region cannot move to the region of the second Brillion, except when there is more energy than the energy of the region forbidden between them.

Table (1) shows the frontiers energies and energy gap (Eg)

Compounds	HOMO(eV)	LUMO(eV)	Eg(eV)
Porphyrin (P)	-5.20119	-2.2842	2.91692
TiTHP	-4.96664	-3.85049	1.116154
TiClTHP	-5.3835	-4.12612	1.257374
TiTPP	-4.53373	-3.42438	1.109352
CdTHP	-6.09014	-3.88259	2.207547
CdClTHP	-6.49992	-4.35523	2.144692
CdTPP	-5.41833	-3.4856	1.932726

Table 1 represents the values of the lowest empty level within the conduction beam and the highest filled level within the valence beam. Energy gap values were also calculated using equation No. 1. The results of the energy gap appear in Table 1. When comparing the energy gap values for porphyrin before and after doping, it can be noted that the energy gap values for all compounds became lower, which is a good result. It is also clear that the value of the energy gap when adding titanium metal to porphyrin is less than the value of the energy gap when adding cadmium metal to porphyrin. This is an important result because all the energy gap values are located in the semiconductor region. It is also important to mention that the obtained energy gap values are very useful, especially in electronic applications such as solar cells and sensors. For example, the value of the energy gap of the compound porphyrin with titanium is similar to the value of the energy gap of silicon. Finally, the lowest value obtained is (1.109352 eV), for the titanium compound with passivation of the phenyl rings.

ResearchJet Journal of Analysis and Inventions
https://reserchjet.academiascience.org

Table(2)the values of ionization potential (I.P), electron affinity (E.A), electronegativity (χ), and electrophilicity (ω).

Structures	I.P(eV)	E.A(eV)	χ (eV)	ω(eV)
Porphyrin (P)	5.20119	2.2842	3.864364	4.80213
TiTHP	4.966641	3.850487	4.408564	17.41293
TiClTHP	5.383499	4.126124	4.754811	17.98042
TiTPP	4.53373	3.424379	3.979054	14.27221
CdTHP	6.090142	3.882595	4.986369	11.26309
CdClTHP	6.499925	4.355233	5.427579	13.73558
CdTPP	5.418327	3.485601	4.451964	10.25492

In Table 2, all values are calculated by using the expression in equations (2, 3, and 7 In fact, the ionization potential and electron affinity are crucial because they can be used to forecast chemical bond strength. They can also be utilized as indicators of whether an atom or molecule will become an electron donor or acceptor. They depend on the type of metal and geometry structure sequent their values become larger or smaller by compare with the value of pure porphyrin. They can also be utilized as indicators of whether an atom or molecule will become an electron donor or acceptor. They depend on the type of metal and geometry structure, so their values become larger or smaller by comparing them with the value of pure porphyrin as shown in table 2. For example, the largest value of I.P and E.A after adding impurities at the electron I.P of Cadmium chlorine meso-tetra(4-phenyl) porphyrin (CdClTPP) is 6.49992 eV, and the structure of CdClTPP has an E.A of 4.355233 eV. On the other hand, the structure with the smallest values of I.P and E.A to the TiTPP structure has I.P (4.53373 eV) and the structure has E.A (3.424379 eV). Furthermore, both I.P. and E.A. are represented as primary bases to predict and obtain other properties. So, it can be used as a sensor device.

The value of the electronegativity for the structure CdClTPP is higher and equal to 5.427579 eV. This means that these structures have a stronger ability to attract the shared electrons. The values of the electrophilicity fluctuate up and down

ResearchJet Journal of Analysis and Inventions
https://reserchjet.academiascience.org

compared to the value of the pristine compound (porphyrin without metal). The reason for changing electrophilicity values is the geometric structure, type, and position of impurities according to the acidity or basicity of Lewis. The values of the electrophilicity fluctuate up and down compared to the value of the porphyrin. Systems doped with porphyrin- (Ti and Cd) have the highest electronegativity values.

Table(3)the values of, softness (σ) , hardness (η), and Fermi level enrgy

SYSYEM	σ(eV)	η(eV)	F.L(eV)
Porphyrin (P)	0.342819	1.46417	-3.86436
TiTHP	0.895934	0.558077	-4.40856
TiClTHP	0.795308	0.628687	-4.75481
TiTPP	0.901428	0.554676	-3.97905
CdTHP	0.452991	1.103774	-4.98637
CdClTHP	0.466267	1.072346	-5.42758
CdTPP	0.517404	0.966363	-4.45196

Depending on previous equations and Table 3, we can see that the energy gap is a function of the chemical hardness. When the structure has a higher value of hardness, it means the structure has a large energy gap. For instance, the porphyrin structure has values for the hardness and energy gap (at ground state), which are equal to (1.46417 eV). Softness is equal to the inverse of the hardness, which leads to the largest value of hardness corresponding to the smallest value of softness, for example, 0.342819 eV and vice versa. In harvesting, hardness and softness are parameters that are very important because they can be used to test both the performance and sensitivity of explosive molecules[35,42]. It is clear that the Fermi level values of metalloporphrin compounds change. These changes in values in comparison with the original porphyrin can be attributed to the crystal structure and the type of metal used. As shown in table 3, For example, the Fermi level values for all structures are lower than the location of the Fermi level for pure porphyrin (-4.02694 eV). Also, one can notice that the lowest value of the Fermi level is for the compound CdClTPP, at -5.42758 eV.

ResearchJet Journal of Analysis and Inventions
https://reserchjet.academiascience.org

4. Conclusions

In this work, the electronic properties of porphyrin and metalloporphyrin were achieved theoretically by using DFT algorithms, the B3LYP technique, and 6-311G (d, p). No imaginary frequency values appeared in the results obtained for all compounds, which means that the results are correct and accurate. Three crucial characteristics must be combined: the first, appropriate structural porphyrin features; the second, an adequate central metal; and the third, suitable metalloporphyrin. Regarding the choice of the central metal, when using a phynol ring and hydrogen, Ti (IVB) and Cd (IIB) are widely accepted as the most suitable central metals. From the metalloporphyrin structure, we can conclude that the best compounds are those that contain titanium atoms in meso-phenyl rings and meso-hydrogen porphyrin (viz: TiTHP and TiTPP). The energy gaps in these structures are the smallest. This result is an important ground state energy gap for all metalloporphyrin compounds located in the semiconducting region, and this gives designers and manufacturers freedom to choose the material and use it in electronic applications. The hardness values of the metalloporphyrin materials are greater than the softness values, which indicates that these compounds are stable.

Acknowledgments

The authors express their appreciation to the PC and Knowledge Networking Center at Thi-Qar University/College of Science for the assistance in facilities for high-performance computing.

Conflicts of Interest: The authors declare no conflicts of interest.

References

1. Hiroto, Y. Miyake, H. Shinokubo, Synthesis and functionalization of porphyrins through organometallic methodologies, Chem. Rev. 117 (2017) 2910–3043.
2. D.R. Roy, E. V Shah, S.M. Roy, Optical activity of Co-porphyrin in the light of IR and Raman spectroscopy: a critical DFT investigation, Spectrochim. Acta Part A Mol. Biomol. Spectrosc. 190 (2018) 121–128.
3. F. Bryden, R.W. Boyle, Metalloporphyrins for medical imaging applications, in: Adv. Inorg. Chem., Elsevier, 2016: pp. 141–221.

ResearchJet Journal of Analysis and Inventions
https://reserchjet.academiascience.org

4. Y. Kabe, M. Ohmori, K. Shinouchi, Y. Tsuboi, S. Hirao, M. Azuma, H. Watanabe, I. Okura, H. Handa, Porphyrin accumulation in mitochondria is mediated by 2-oxoglutarate carrier, J. Biol. Chem. 281 (2006) 31729–31735.
5. M.E. Önal, MOLECULAR MAGNETIC MATERIALS BASED ON PORPHYRIN MACROCYCLES, (2014).
6. G. Zamborlini, M. Jugovac, A. Cossaro, A. Verdini, L. Floreano, D. Lüftner, P. Puschnig, V. Feyer, C.M. Schneider, On-surface nickel porphyrin mimics the reactive center of an enzyme cofactor, Chem. Commun. 54 (2018) 13423–13426.
7. H.D. Pranowo, F. Mulya, H.A. Aziz, G.A. Santoso, Study of substituent effect on properties of Platinum (II) porphyrin semiconductor using density functional theory, Indones. J. Chem. 18 (2018) 742–748.
8. M. Cao, A. Gao, Y. Liu, Y. Zhou, Z. Sun, Y. Li, F. He, L. Li, L. Mo, R. Liu, Theoretical study on electronic structural properties of catalytically reactive metalloporphyrin intermediates, Catalysts. 10 (2020) 224.
9. D.K. Deda, B.A. Iglesias, E. Alves, K. Araki, C.R.S. Garcia, Porphyrin derivative nanoformulations for therapy and antiparasitic agents, Molecules. 25 (2020) 2080.
10. J.M. Gallego, Macrocycle metalation on solid surfaces, (2018).
11. R. Chen, Y. Wang, Y. Ma, A. Mal, X.-Y. Gao, L. Gao, L. Qiao, X.-B. Li, L.-Z. Wu, C. Wang, Rational design of isostructural 2D porphyrin-based covalent organic frameworks for tunable photocatalytic hydrogen evolution, Nat. Commun. 12 (2021) 1–9.
12. C.-R. Zhang, L.-H. Han, J.-W. Zhe, N.-Z. Jin, Y.-L. Shen, J.-J. Gong, H.-M. Zhang, Y.-H. Chen, Z.-J. Liu, The role of terminal groups in electronic structures and related properties: The case of push–pull porphyrin dye sensitizers for solar cells, Comput. Theor. Chem. 1039 (2014) 62–70.
13. F. Mulya, G.A. Santoso, H.A. Aziz, H.D. Pranowo, Design a better metalloporphyrin semiconductor: A theoretical studies on the effect of substituents and central ions, in: AIP Conf. Proc., AIP Publishing LLC, 2016: p. 80006.
14. H.A. Aziz, G.A. Santoso, F. Mulya, H.D. Pranowo, Molecular and electronic structure of some symmetrically meso-substituted Hg (II)-porphyrin complexes, Asian J. Chem. 29 (2017) 2224–2226.

ResearchJet Journal of Analysis and Inventions
https://reserchjet.academiascience.org

15. A.S. Shalabi, M.M. Assem, K.A. Soliman, A.M. El Mahdy, H.O. Taha, Performance of metalloporphyrin malonic acids as dye sensitizers for use in dye-sensitized solar cells assessed by density functional theory, Mater. Sci. Semicond. Process. 26 (2014) 119–129.
16. J. Barbee, A.E. Kuznetsov, Revealing substituent effects on the electronic structure and planarity of Ni-porphyrins, Comput. Theor. Chem. 981 (2012) 73–85.
17. U. Utari, K. Kusumandari, B. Purnama, M. Mudasir, K. Abraha, Surface Morphology of Fe (III)-Porphyrin Thin Layers as Characterized by Atomic Force Microscopy, Indones. J. Chem. 16 (2016) 233–238.
18. G. Harrach, Z. Valicsek, O. Horváth, Water-soluble silver (II) and gold (III) porphyrins: The effect of structural distortion on the photophysical and photochemical behavior, Inorg. Chem. Commun. 14 (2011) 1756–1761.
19. W. Zheng, N. Shan, L. Yu, X. Wang, UV–visible, fluorescence and EPR properties of porphyrins and metalloporphyrins, Dye. Pigment. 77 (2008) 153–157.
20. X.-F. Wang, J. Xiang, P. Wang, Y. Koyama, S. Yanagida, Y. Wada, K. Hamada, S. Sasaki, H. Tamiaki, Dye-sensitized solar cells using a chlorophyll a derivative as the sensitizer and carotenoids having different conjugation lengths as redox spacers, Chem. Phys. Lett. 408 (2005) 409–414.
21. M.S. Seo, N.H. Kim, K.-B. Cho, J.E. So, S.K. Park, M. Clémancey, R. Garcia-Serres, J.-M. Latour, S. Shaik, W. Nam, A mononuclear nonheme iron (IV)-oxo complex which is more reactive than cytochrome P450 model compound I, Chem. Sci. 2 (2011) 1039–1045.
22. J.W. Shin, S.R. Rowthu, M.Y. Hyun, Y.J. Song, C. Kim, B.G. Kim, K.S. Min, Monomeric, trimeric, and tetrameric transition metal complexes (Mn, Fe, Co) containing N, N-bis (2-pyridylmethyl)-2-aminoethanol/-ate: preparation, crystal structure, molecular magnetism and oxidation catalysis, Dalt. Trans. 40 (2011) 5762–5773.
23. W. Liu, J.T. Groves, Manganese porphyrins catalyze selective C– H bond halogenations, J. Am. Chem. Soc. 132 (2010) 12847–12849.
24. M.M. Pereira, L.D. Dias, M.J.F. Calvete, Metalloporphyrins: bioinspired oxidation catalysts, Acs Catal. 8 (2018) 10784–10808.
25. S. Yamazaki, Metalloporphyrins and related metallomacrocycles as electrocatalysts for use in polymer electrolyte fuel cells and water

ResearchJet Journal of Analysis and Inventions
https://reserchjet.academiascience.org

electrolyzers, Coord. Chem. Rev. 373 (2018) 148–166.
26. G.-P. Yan, D. Bischa, S.E. Bottle, Synthesis and properties of novel porphyrin spin probes containing isoindoline nitroxides, Free Radic. Biol. Med. 43 (2007) 111–116.
27. M.L. Jabbar, K.J. Kadhim, Linear & nonlinear optical properties of undoped & doped graphene nanoribbon via TD-DFT study, AIP Conf. Proc. 2292 (2020). https://doi.org/10.1063/5.0030597.
28. N.H. Al-Saadawy, Synthesis, Characterization and Theoretical Studies of New Organotellurium Compounds Based on (4-(((1S, E)-1, 7, 7-trimethylbicyclo [2.2. 1] heptan-2-ylidene) amino) phenyl) mercury (II) Chloride, Indones. J. Chem. (2021).
29. M.L. Jabbar, Theoretical study for the interactions of Coronene-Y interactions by using Density functional theory with hybrid function, Univ. Thi-Qar J. 13 (2018) 28–41.
30. A.D. Becke, Density-functional thermochemistry. II. The effect of the Perdew–Wang generalized-gradient correlation correction, J. Chem. Phys. 97 (1992) 9173–9177.
31. M. H Muzel, A.S. Alwan, M.L. Jabbar, Electronical Properties for (CxHyZ2-NO) Nanoclusters, Curr. Nanomater. 2 (2017) 33–38.
32. M.L. Jabbar, K.J. Kadhim, Electronic Properties of Doped Graphene Nanoribbon and the Electron Distribution Contours: A DFT Study, Russ. J. Phys. Chem. B. 15 (2021) 46–52.
33. C. Lee, W. Yang, R.G. Parr, Development of the Colle-Salvetti correlation-energy formula into a functional of the electron density, Phys. Rev. B. 37 (1988) 785.
34. A.S. Alwan, Density functional theory investigation of (C4H2N2) 3 nanocluster and (C4H2N2) 3--P, Al, As, B, C and in nanoclusters, in: AIP Conf. Proc., AIP Publishing LLC, 2020: p. 30013.
35. M.L. Jabbar, Computational studies on electronic and optical properties of dopamine derivatives structure: A DFT study, J. Mech. Behav. Mater. 30 (2021) 279–284.
36. N.M. O'boyle, A.L. Tenderholt, K.M. Langner, Cclib: a library for package-independent computational chemistry algorithms, J. Comput. Chem. 29 (2008) 839–845.
37. M.L. Jabbar, Some electronical properties for Coronene-Y interactions by using

ResearchJet Journal of Analysis and Inventions
https://reserchjet.academiascience.org

density functional theory (DFT), J. Basrah Res. 44 (2018) 11–19.
38. A.S. Alwan, S.K. Ajeel, M.L. Jabbar, Theoretical study for Coronene and Coronene-Al, B, C, Ga, In and Coronene-O interactions by using Density Functional theory, Univesity Thi-Qar J. 14 (2019).
39. V.P. Gupta, Principles and applications of quantum chemistry, Academic Press, 2015.
40. R. Vivas-Reyes, A. Aria, Evaluation of group electronegativities and hardness (softness) of group 14 elements and containing functional groups through density functional theory and correlation with NMR spectra data, Eclética Química. 33 (2008) 69–76.
41. M. Frisch, G.W. Trucks, H.B. Schlegel, G.E. Scuseria, M.A. Robb, J.R. Cheeseman, G. Scalmani, V. Barone, B. Mennucci, Ga. Petersson, Gaussian 09, revision D. 01, (2009).
42. G.W. Ejuh, M.T.O. Abe, F.T. Nya, J.M.B. Ndjaka, Prediction of electronic structure, dielectric and thermodynamical properties of flurbiprofen by density functional theory calculation, Karbala Int. J. Mod. Sci. 4 (2018) 12–20.